Int. J. Solids Structures Vol. 21, No. 7, pp. 617–643, 1985
Printed in Great Britain.

0020-7683/85 $3.00 + .00

DYNAMICS OF A BEAM MOVING OVER SUPPORTS

KEITH W. BUFFINTON and THOMAS R. KANE
Division of Applied Mechanics, Stanford University, Stanford, CA 94305, U.S.A.

Abstract—The behavior of a uniform beam moving longitudinally at a prescribed rate over two bilateral supports is studied. Equations of motion are formulated by regarding the supports as kinematical constraints imposed on an unrestrained beam and by discretizing the beam via the assumed modes technique. The results of numerical simulations are displayed for cases in which the beam undergoes no longitudinal motion, sinusoidal longitudinal motion, or longitudinal motion for the purpose of repositioning. The instability of harmonic longitudinal motion is investigated, and methods are presented for predicting whether or not a given motion will give rise to an unstable response.

INTRODUCTION

Figure 1 displays an elastic, uniform beam B capable of deflecting transversely while moving longitudinally at a prescribed rate over two bilateral supports. Figure 2 shows a plot of the transverse displacement of the endpoint H of B when B is undergoing a longitudinal motion which varies sinusoidally with time. A similar plot of the motion of H, applicable when the longitudinal motion of B is again sinusoidal, but at a different frequency, is shown in Fig. 3. The primary purpose of this study is to detail methodologies both for efficiently generating plots such as those in Figs. 2 and 3 and for predicting, in advance of their generation, qualitative differences between them.

The responses of beams in situations similar to the one depicted in Fig. 1 have been studied extensively. For example, beams acted upon by known forces whose points of application vary with time are discussed in many standard texts, such as [1]. The responses of beams undergoing overall motions relative to a fixed reference frame are also well known[1], and have many practical applications in the field of earthquake engineering. Less well known, but important in connection with band saw blades and high-speed computer tapes, are the solutions to problems involving beams of infinite length moving at a constant rate over supports[2, 3]. The problem at hand differs from all of these in several respects. First, the forces exerted on the beam by the supports have magnitudes that depend on the motion of the beam; thus, they are *unknown*. Second, the beam moves not only relative to an inertial reference frame but also relative to its supports. Finally, the length of the beam is finite, and the rate of the beam's longitudinal motion is arbitrary. The problem of a cantilever beam whose length varies with time, studied in [4], shares these distinguishing characteristics; however, the system shown in Fig. 1 has not previously been the subject of investigation.

The steps taken in developing equations of motion are detailed in the following section, entitled Equations of Motion. Next, the results of numerical simulations are presented to illustrate the response of the beam when it undergoes no longitudinal motion, sinusoidal longitudinal motion, and longitudinal motion performed for the purpose of repositioning. Information relevant to the instability of periodic longitudinal motion, developed by making use of Floquet's theory[5] and results reported by Hsu[6], then appears under the heading Instability of Periodic Motion. Finally, elaborative comments are presented.

EQUATIONS OF MOTION

The result of the ensuing analysis is a set of equations to be used to simulate the motion of a beam moving longitudinally over supports. The assumptions made in the development of these equations are that transverse deformations are both "small" and adequately described by Bernoulli-Euler beam theory (i.e. shear deformations and ro-

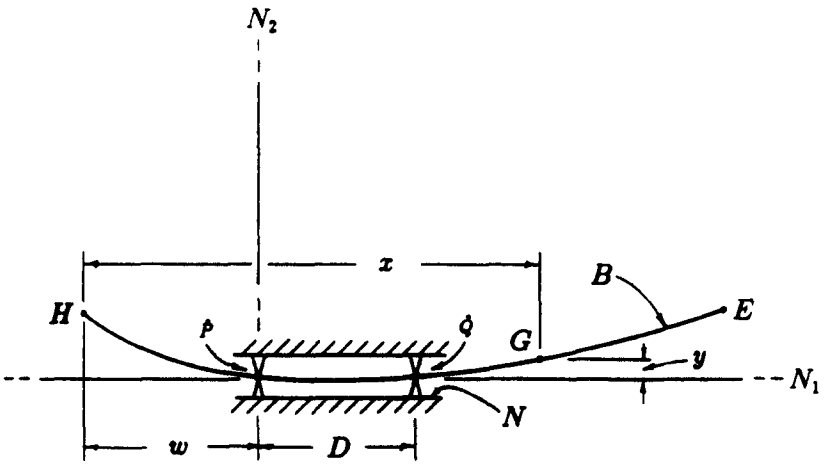

Fig. 1. Beam moving over supports.

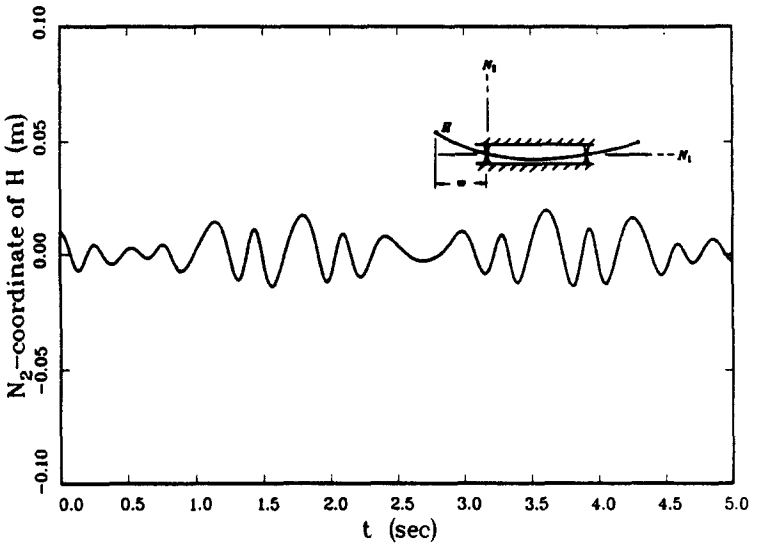

Fig. 2. Sinusoidal longitudinal motion with $w = 0.375 - 0.05 \sin 10.0t$ m.

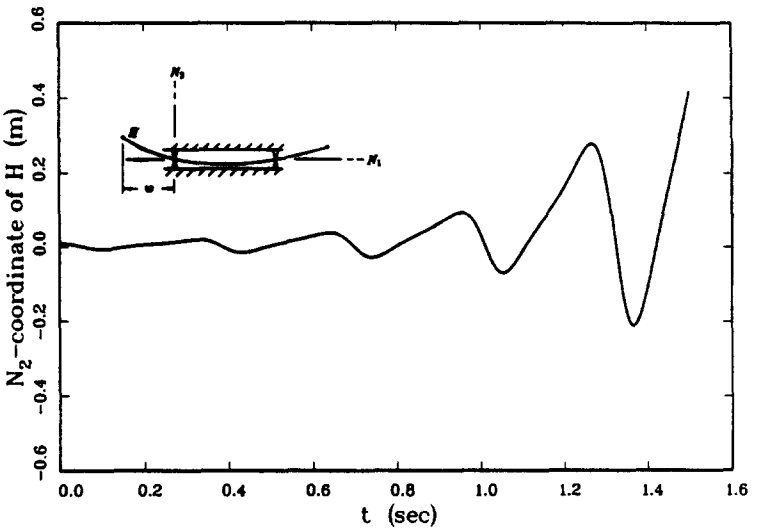

Fig. 3. Sinusoidal longitudinal motion with $w = 0.375 - 0.05 \sin 20.0t$ m.

tatory inertia are neglected), that axial deformations are ignorable, and that all motions, both longitudinal and transverse, take place in a single plane. The equations are formulated by regarding the supports as kinematical constraints imposed on an unrestrained beam, by using assumed modes[7] to discretize the beam, and by applying Kane's method[8] cast in the alternate form presented in [9].

System geometry

The beam B of Fig. 1 is supported at points $\hat{P}$ and $\hat{Q}$ of a line N_1 fixed in an inertial reference frame N. Line N_2, also fixed in N, is perpendicular to N_1 and passes through $\hat{P}$. All motions of B are confined to the N_1–N_2 plane, regarded as horizontal so that gravity may be neglected. The distance between $\hat{P}$ and $\hat{Q}$ is D, and the prescribed, time-dependent distance between $\hat{P}$ and the endpoint H of B is w. The endpoint of B opposite H is designated E. The distance, as measured along N_1, from H to a generic point G of B is x, while the perpendicular distance from N_1 to G is y.

In Fig. 4, B is shown free of supports and in a general configuration in the N_1–N_2 plane. This representation facilitates the formulation of equations of motion and, as is discussed in greater detail in the Elaborative Comments, permits the formulation of a set of equations that can be integrated numerically in a particularly efficient manner. To this end, one can introduce, in a way similar to that used in [10], an auxiliary reference frame R defined by the mutually perpendicular lines R_1 and R_2 intersecting at a point R^* and lying in the N_1–N_2 plane. The position of R^* relative to $\hat{P}$ is characterized by z_1 and z_2, as depicted, while the orientation of R in N is described by the angle θ between N_1 and R_1. The R_1-coordinate and R_2-coordinate of G are ξ and η, respectively, and the angle between R_1 and the tangent to B at G is α. Finally, P is the point on B that lies on N_2, while Q is the point on B that lies on a line parallel to N_2 passing through $\hat{Q}$.

Kinematics

To write the equations governing motions of B as a set of ordinary, rather than partial, differential equations, we express η in terms of "modal" functions ϕ_i as

$$\eta(s, t) = \sum_{i=1}^{\nu} \phi_i(s) q_i(t), \tag{1}$$

where $\phi_i (i = 1, \ldots, \nu)$ are, as yet, unrestricted functions of s, the arc length as measured along B from H to G, $q_i (i = 1, \ldots, \nu)$ are functions of time t, and ν is a positive integer. The quantities α and ξ can be expressed in terms of ϕ_i and q_i by means

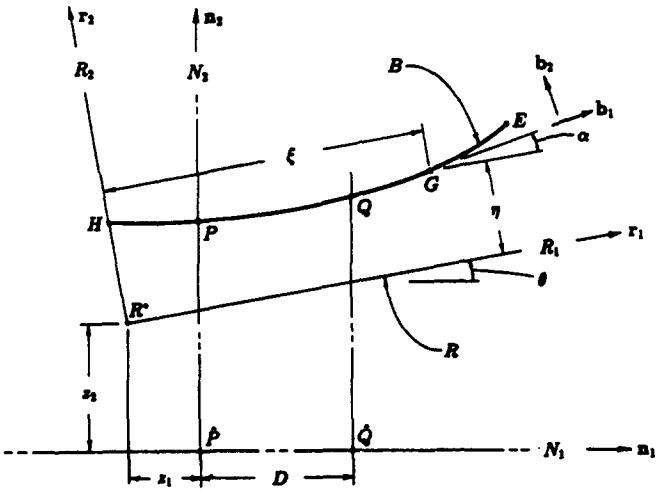

Fig. 4. Beam free of supports.

of the relations

$$\frac{\partial \xi(s, t)}{\partial s} = \cos \alpha(s, t), \tag{2}$$

$$\frac{\partial \eta(s, t)}{\partial s} = \sin \alpha(s, t), \tag{3}$$

and

$$\sin^2 \alpha + \cos^2 \alpha = 1. \tag{4}$$

Thus, once ϕ_i and q_i are known, one has a complete description of the configuration of B in R. Since three additional quantities, namely z_1, z_2, and θ, are needed to fix the position and orientation of R in N, B possesses $\nu + 3$ degrees of freedom in N. Correspondingly, generalized speeds $u_i (i = 1, \ldots, \nu + 3)$ are introduced as

$$\begin{aligned} u_i &\triangleq \dot{q} \qquad (i = 1, \ldots, \nu), \\ u_{\nu+1} &\triangleq \mathbf{v}^{R^*} \cdot \mathbf{n}_1 = -\dot{z}_1, \\ u_{\nu+2} &\triangleq \mathbf{v}^{R^*} \cdot \mathbf{n}_2 = \dot{z}_2, \\ u_{\nu+3} &\triangleq \boldsymbol{\omega}^R \cdot \mathbf{n}_3 = \dot{\theta}, \end{aligned} \tag{5}$$

where $\mathbf{v}^{R^*}$ is the velocity of R^* in N, $\boldsymbol{\omega}^R$ is the angular velocity of R in N, and $\mathbf{n}_1$, $\mathbf{n}_2$, and $\mathbf{n}_3$ are elements of a dextral set of unit vectors such that $\mathbf{n}_1$ and $\mathbf{n}_2$ are directed as shown in Fig. 4, and $\mathbf{n}_3 = \mathbf{n}_1 \times \mathbf{n}_2$. The velocity of G in N is written as

$$\begin{aligned} \mathbf{v}^G = &\left(\frac{\partial \xi}{\partial t} + c_\theta u_{\nu+1} + s_\theta u_{\nu+2} - \eta u_{\nu+3} \right) \mathbf{r}_1 \\ &+ \left(\frac{\partial \eta}{\partial t} - s_\theta u_{\nu+1} + c_\theta u_{\nu+2} + \xi u_{\nu+3} \right) \mathbf{r}_2, \end{aligned} \tag{6}$$

where $s_\theta \triangleq \sin \theta$, $c_\theta \triangleq \cos \theta$, and $\mathbf{r}_1$ and $\mathbf{r}_2$ are unit vectors directed as shown in Fig. 4. To be able to use this equation to form partial velocities, one must express $\partial \xi / \partial t$ and $\partial \eta / \partial t$ in terms of $u_i (i, \ldots, \nu + 3)$. For $\partial \xi / \partial t$, this is easily accomplished by differentiating eqn (1) with respect to t and by then utilizing eqns (5). For $\partial \xi / \partial t$, one first makes use eqn (2) to obtain

$$\xi = \int_0^s \cos \alpha(\sigma, t)\, d\sigma. \tag{7}$$

Taking advantage of the fact that $\dot{s} = 0$, one then differentiates this equations with respect to t to produce

$$\frac{\partial \xi}{\partial t} = \int_0^s \frac{\partial \cos \alpha(\sigma, t)}{\partial t}\, d\sigma. \tag{8}$$

Next, differentiation of eqn (4) yields

$$\frac{\partial \cos \alpha}{\partial t} = -\tan \alpha \frac{\partial \sin \alpha}{\partial t}, \tag{9}$$

which, in view of eqns (1), (3), and (5), leads to

$$\frac{\partial \cos \alpha}{\partial t} = -\tan \alpha \sum^{\nu} \phi_i' u_i. \tag{10}$$

Finally, substituting from eqn (10) into eqn (8) and then substituting the result, along with the expression for $\partial\eta/\partial t$ obtained by differentiating eqn (1), into eqn (6) yields

$$\mathbf{v}^G = \left\{ -\sum_{i=1}^{\nu} \left[\int_0^s \phi_i'(\sigma) \tan \alpha(\sigma, t)\, d\sigma \right] u_i + c_\theta u_{\nu+1} + s_\theta u_{\nu+2} - \eta u_{\nu+3} \right\} \mathbf{r}_1 + \left(\sum_{i=1}^{\nu} \phi_i u_i - s_\theta u_{\nu+1} + c_\theta u_{\nu+2} + \xi u_{\nu+3} \right) \mathbf{r}_2. \quad (11)$$

Partial velocities of G in N, formed by inspection of eqn (11), are

$$\begin{aligned} \mathbf{v}_i^G &= -\left[\int_0^s \phi_i'(\sigma) \tan \alpha(\sigma, t)\, d\sigma \right] \mathbf{r}_1 + \phi_i \mathbf{r}_2 \qquad (i = \ldots, \nu), \\ \mathbf{v}_{\nu+1}^G &= c_\theta \mathbf{r}_1 - s_\theta \mathbf{r}_2, \\ \mathbf{v}_{\nu+2}^G &= s_\theta \mathbf{r}_1 + c_\theta \mathbf{r}_2, \\ \mathbf{v}_{\nu+3}^G &= -\eta \mathbf{r}_1 + \xi \mathbf{r}_2. \end{aligned} \quad (12)$$

So far, all expressions have been written in their full nonlinear form. This is in accordance with the precepts of Kane's method, which permit linearization of kinematical expressions only after partial velocities have been identified. Since equations of motion governing only "small" displacements of B from N_1 are desired, linearization of all expressions in the quantities $q_i (i = 1, \ldots, \nu)$, z_2, θ, $u_i (i = 1, \ldots, \nu)$, $u_{\nu+2}$, and $u_{\nu+3}$ is now appropriate. Consequently, by making use of eqns (1–4), we write

$$\xi = s, \quad (13)$$

$$\eta(\xi, t) = \sum_{i=1}^{\nu} \phi_i(\xi) q_i(t), \quad (14)$$

$$\alpha(\xi, t) = \sum_{i=1}^{\nu} \phi_i'(\xi) q_i(t), \quad (15)$$

and replace eqns (11) and (12) with

$$\mathbf{v}^G = u_{\nu+1} \mathbf{r}_1 + \left(\sum_{i=1}^{\nu} \phi_i u_i - \theta u_{\nu+1} + u_{\nu+2} + \xi u_{\nu+3} \right) \mathbf{r}_2, \quad (16)$$

and

$$\begin{aligned} \mathbf{v}_i^G &= -\sum_{j=1}^{\nu} \epsilon_{ij} q_j \mathbf{r}_1 + \phi_i \mathbf{r}_2 \qquad (i = 1, \ldots, \nu), \\ \mathbf{v}_{\nu+1}^G &= \mathbf{r}_1 - \theta \mathbf{r}_2, \\ \mathbf{v}_{\nu+2}^G &= \theta \mathbf{r}_1 + \mathbf{r}_2, \\ \mathbf{v}_{\nu+3}^G &= -\eta \mathbf{r}_1 + \xi \mathbf{r}_2, \end{aligned} \quad (17)$$

where

$$\epsilon_{ij}(\xi) \triangleq \int_0^\xi \phi_i'(\sigma) \phi_j'(\sigma)\, d\sigma \qquad (i, j = 1, \ldots, \nu). \quad (18)$$

Note that if linearization had been performed prematurely, and partial velocities had been obtained from a linearized expression for the velocity of G, as in eqn (16), then terms involving $\epsilon_{ij} (i, j = 1, \ldots, \nu)$ would have been lost. The importance of ensuring

that these terms appear in the equations governing the motion of B is demonstrated in the upcoming section entitled Simulations.

The linearized acceleration of G in N is constructed by differentiating $\mathbf{v}^G$, as given in eqn (16), with respect to time in N, which leads to

$$\mathbf{a}^G = \dot{u}_{\nu+1}\mathbf{r}_1 + \left(\sum_{i=1}^{\nu} \phi_i \dot{u}_i - \theta \dot{u}_{\nu+1} + \dot{u}_{\nu+2} + \xi \dot{u}_{\nu+3}\right)\mathbf{r}_2. \tag{19}$$

Generalized forces

The generalized inertia forces F_r^* associated with the generalized speeds $u_r (r = 1, \ldots, \nu + 3)$ are given by

$$F_r^* = \int_0^L \mathbf{v}_r^G \cdot (-\rho \mathbf{a}^G)\, d\xi \qquad (r = 1, \ldots, \nu + 3), \tag{20}$$

where L and ρ denote the length and the mass per unit length of B, respectively. After defining constants m, e, J, a_{ij}, b_{ij}, c_i, and d_i as

$$m \triangleq \rho L, \qquad e \triangleq \frac{\rho L^2}{2}, \qquad J \triangleq \frac{\rho L^3}{3}, \tag{21}$$

and

$$\left.\begin{aligned} a_{ij} &\triangleq \rho \int_0^L \phi_i(\xi)\phi_j(\xi)\, d\xi, \\ b_{ij} &\triangleq \rho \int_0^L \epsilon_{ij}(\xi)\, d\xi, \\ c_i &\triangleq \rho \int_0^L \phi_i(\xi)\, d\xi, \\ d_i &\triangleq \rho \int_0^L \xi\phi_i(\xi)\, d\xi, \end{aligned}\right\} \qquad (i, j = 1, \ldots, \nu) \tag{22}$$

one can substitute from eqns (17) and (19) into eqn (20) to obtain

$$F_j^* = -\sum_{i=1}^{\nu} a_{ij}\dot{u}_i + \left(\sum_{i=1}^{\nu} b_{ij}q_i + c_j\theta\right)\dot{u}_{\nu+1} - c_j\dot{u}_{\nu+2} - d_j\dot{u}_{\nu+3} \qquad (j = 1, \ldots, \nu), \tag{23}$$

$$F_{\nu+1}^* = -m\dot{u}_{\nu+1}, \tag{24}$$

$$F_{\nu+2}^* = -\sum_{i=1}^{\nu} c_i\dot{u}_i - m\dot{u}_{\nu+2} - e\dot{u}_{\nu+3}, \tag{25}$$

$$F_{\nu+3}^* = -\sum_{i=1}^{\nu} d_i\dot{u}_i + \left(\sum_{i=1}^{\nu} c_iq_i + e\theta\right)\dot{u}_{\nu+1} - e\dot{u}_{\nu+2} - J\dot{u}_{\nu+3}. \tag{26}$$

The only contributions to the generalized active forces $F_r (r = 1, \ldots, \nu + 3)$ are due to deformations of B and are constructed by making use of a strain energy function V. For a uniform Bernoulli-Euler beam, V is given by

$$V = \frac{1}{2} EI \int_0^L \left(\frac{\partial^2 \eta}{\partial \xi^2}\right)^2 d\xi, \tag{27}$$

where E and I are the modulus of elasticity and cross-sectional moment of inertia of B, respectively. After substituting from eqn (1) into eqn (27), one obtains the first ν

generalized active forces from

$$F_j = -\frac{\partial V}{\partial q_j} \qquad (j = 1, \ldots, \nu), \tag{28}$$

while the remaining generalized active forces are all equal to zero. Consequently,

$$F_j = -\sum_{i=1}^{\nu} h_{ij} q_i \qquad (j = 1, \ldots, \nu), \tag{29}$$

$$F_{\nu+1} = F_{\nu+2} = F_{\nu+3} = 0, \tag{30}$$

where h_{ij} is defined as

$$h_{ij} \triangleq EI \int_0^L \phi_i''(\xi)\phi_j''(\xi)\, d\xi \qquad (i, j = 1, \ldots, \nu). \tag{31}$$

Constraint equations

Equations (23–26), (29), and (30) could be used at this point, in conjunction with Kane's equations, to obtain the dynamical equations governing unrestrained motions of B. The equations of interest, however, are those that govern motions of B when B is constrained to remain in contact with the supports at points $\hat{P}$ and $\hat{Q}$. These equations will be formulated by first developing constraint equations expressed in terms of the generalized speeds and by then making use of the procedure described in [9]. The constraint equations are obtained by setting the $\mathbf{n}_1$ component of the velocity of H equal to $-\dot{w}\mathbf{n}_1$ and the time derivatives of the $\mathbf{n}_2$ components of the position vectors of P and Q relative to $\hat{P}$ equal to zero. That is,

$$\mathbf{v}^H \cdot \mathbf{n}_1 = -\dot{w}, \tag{32}$$

$$\frac{d}{dt}(\mathbf{p}^{\hat{P}P} \cdot \mathbf{n}_2) = 0, \tag{33}$$

$$\frac{d}{dt}(\mathbf{p}^{\hat{P}Q} \cdot \mathbf{n}_2) = 0, \tag{34}$$

where $\mathbf{v}^H$ is the velocity of H in N, and $\mathbf{p}^{\hat{P}P}$ and $\mathbf{p}^{\hat{P}Q}$ are the position vectors from $\hat{P}$ to P and Q, respectively. With $s = 0$, eqn (11) yields an expression for $\mathbf{v}^H$; hence, eqn (32) leads to

$$-s_\theta \sum_{i=1}^{\nu} \phi_i(0) u_i + u_{\nu+1} - c_\theta u_{\nu+3} \sum_{i=1}^{\nu} \phi_i(0) q_i = -\dot{w}. \tag{35}$$

To construct the constraint equations implied by eqns (33) and (34), we begin by using eqns (1) and (2) to develop expressions for the quantities ξ^P, η^P, ξ^Q, and η^Q, which represent the values of ξ and η corresponding to the positions of P and Q. These are

$$\xi^P(s^P, t) \triangleq \int_0^{s^P} \cos\alpha(\sigma, t)\, d\sigma, \tag{36}$$

$$\eta^P(s^P, t) \triangleq \sum_{i=1}^{\nu} \phi_i(s^P) q_i(t), \tag{37}$$

$$\xi^Q(s^Q, t) \triangleq \int_0^{s^Q} \cos\alpha(\alpha, t)\, d\sigma, \tag{38}$$

$$\eta^Q(s^Q, t) \triangleq \sum_{i=1}^{\nu} \phi_i(s^Q) q_i(t), \tag{39}$$

where s^P and s^Q are the arc lengths, measured along B, from H to P and from H to Q, respectively. Note that since P and Q are not fixed on B, s^P and s^Q are not independent variables, but are functions of time. After developing expressions for $\mathbf{p}^{PP}$ and $\mathbf{p}^{PQ}$, utilizing eqns (36–39), and then substituting from the resulting expressions into eqns (33) and (34), one arrives at the constraint equations as

$$u_{\nu+2} - (s_\theta \eta^P - c_\theta \xi^P) u_{\nu+3} + s_\theta \frac{d\xi^P}{dt} + c_\theta \frac{d\eta^P}{dt} = 0, \tag{40}$$

$$u_{\nu+2} - (s_\theta \eta^Q - c_\theta \xi^Q) u_{\nu+3} + s_\theta \frac{d\xi^Q}{dt} + c_\theta \frac{d\eta^Q}{dt} = 0. \tag{41}$$

Before one can use eqns (40) and (41) to construct the dynamical equations governing constrained motions of B, one must express them in a form such that the generalized speeds $u_1, \ldots, u_{\nu+3}$ appear explicitly. Consider for the moment only eqn (40). By differentiating eqns (36) and (37) with respect to time, using Leibnitz's rule[11], and by utilizing eqns (1–4), one obtains

$$\frac{d\xi^P}{dt} = -\sum_{i=1}^{\nu} \left[\int_0^{s^P} \phi_i'(\sigma) \tan \alpha(\sigma, t)\, d\sigma \right] u_i + \cos \alpha^P \frac{ds^P}{dt}, \tag{42}$$

$$\frac{d\eta^P}{dt} = \sum_{i=1}^{\nu} \phi_i(s^P) u_i + \sin \alpha^P \frac{ds^P}{dt}, \tag{43}$$

where α^P denotes the value of $\alpha(s, t)$ evaluated for $s = s^P$. The geometry of Fig. 4 reveals that

$$\xi^P = \eta^P \tan \theta + \frac{z_1}{c_\theta}. \tag{44}$$

After differentiating this equation with respect to t and making use of eqns (5), one concludes that

$$\frac{d\xi^P}{dt} = \tan \theta \frac{d\eta^P}{dt} - \frac{1}{c_\theta} u_{\nu+1} + \frac{1}{c_\theta^2} (s_\theta z_1 + \eta^P) u_{\nu+3}. \tag{45}$$

Using eqns (42–45) in conjunction with eqn (40), one thus arrives at a constraint equation expressed explicitly in terms of the generalized speeds $u_i (i = 1, \ldots, \nu + 3)$ as

$$\sum_{i=1}^{\nu} \left[\sin \alpha^P \int_0^{s^P} \phi_i'(\sigma) \tan \alpha(\sigma, t)\, d\sigma + \phi_i(s^P) \cos \alpha^P \right] u_i - (s_\theta \cos \alpha^P + c_\theta \sin \alpha^P) u_{\nu+1} + (c_\theta \cos \alpha^P - s_\theta \sin \alpha^P) u_{\nu+2} + (\eta^P \sin \alpha^P + \xi^P \cos \alpha^P) u_{\nu+3} = 0. \tag{46}$$

Similarly, Eq. (41) implies

$$\sum_{i=1}^{\nu} \left[\sin \alpha^Q \int_0^{s^Q} \phi_i'(\sigma) \tan \alpha(\sigma, t)\, d\sigma + \phi_i(s^Q) \cos \alpha^Q \right] u_i - (s_\theta \cos \alpha^Q + c_\theta \sin \alpha^Q) u_{\nu+1} + (c_\theta \cos \alpha^Q - s_\theta \sin \alpha^Q) u_{\nu+2} + (\eta^Q \sin \alpha^Q + \xi^Q \cos \alpha^Q) u_{\nu+3} = 0. \tag{47}$$

It is interesting to note that, with eqns (46) and (47) in hand, one can show that eqns (33) and (34) are equivalent to

$$\mathbf{v}^P \cdot \mathbf{b}_2^P = 0, \tag{48}$$

$$\mathbf{v}^Q \cdot \mathbf{b}^{Q_2} = 0, \tag{49}$$

where $\mathbf{v}^{\dot{P}}$ and $\mathbf{v}^{\dot{Q}}$ are the velocities, in N, of points *fixed* on B and located at positions instantaneously coinciding with the positions of P and Q, and $\mathbf{b}_2^P$ and $\mathbf{b}_2^Q$ are unit vectors normal to B at P and Q, respectively. Unfortunately, this fact only becomes apparent after eqns (46) and (47) are available, and consequently eqns (48) and (49) do not provide a viable approach for generating eqns (46) and (47) directly from eqn (11).

Equations (35), (46) and (47) can be expressed in the matrix form

$$\underline{A}\,\underline{u} + \underline{B} = \underline{0}, \tag{50}$$

where $\underline{A}$ is a $3 \times (\nu + 3)$ matrix, $\underline{u}$ is a $(\nu + 3) \times 1$ matrix of generalized speeds, and $\underline{B}$ is a 3×1 matrix. The elements of $\underline{A}$ and $\underline{B}$, identified by reference to eqns (35), (46) and (47), are

$$\begin{aligned}
A_{1i} &= -s_\theta \phi_i(0) \qquad (i = 1, \ldots, \nu),\\
A_{1\nu+1} &= 1,\\
A_{1\nu+2} &= 0,\\
A_{1\nu+3} &= -c_\theta \sum_{i=1}^{\nu} \phi_i(0) q_i,\\
A_{2i} &= \sin\alpha^P \int_0^{s^P} \phi_i'(\sigma) \tan\alpha(\sigma, t)\, d\sigma + \phi_i(s^P) \cos\alpha^P \qquad (i = 1, \ldots, \nu),\\
A_{2\nu+1} &= -s_\theta \cos\alpha^P - c_\theta \sin\alpha^P,\\
A_{2\nu+2} &= c_\theta \cos\alpha^P - s_\theta \sin\alpha^P,\\
A_{2\nu+3} &= \eta^P \sin\alpha^P + \xi^P \cos\alpha^P,\\
A_{3i} &= \sin\alpha^Q \int_0^{s^Q} \phi_i'(\sigma) \tan\alpha(\sigma, t)\, d\sigma + \phi_i(s^Q) \cos\alpha^Q \qquad (i = 1, \ldots, \nu),\\
A_{3\nu+1} &= -s_\theta \cos\alpha^Q - c_\theta \sin\alpha^Q,\\
A_{3\nu+2} &= c_\theta \cos\alpha^Q - s_\theta \sin\alpha^Q,\\
A_{3\nu+3} &= \eta^Q \sin\alpha^Q + \xi^Q \cos\alpha^Q,
\end{aligned} \tag{51}$$

$$\begin{aligned}
B_1 &= \dot{w},\\
B_2 &= 0,\\
B_3 &= 0.
\end{aligned} \tag{52}$$

Linearization of eqns (35), (46), (47), (51) and (52) in the variables $q_i (i = 1, \ldots, \nu)$, z_2, θ, $u_i (i = 1, \ldots, \nu)$, $u_{\nu+2}$ and $u_{\nu+3}$ yields

$$u_{\nu+1} = -\dot{w}, \tag{53}$$

$$\sum_{i=1}^{\nu} \phi_i(w) u_i - \left[\theta + \sum_{i=1}^{\nu} \phi_i'(w) q_i\right] u_{\nu+1} + u_{\nu+2} + w u_{\nu+3} = 0, \tag{54}$$

$$\sum_{i=1}^{\nu} \phi_i(w + D) u_i - \left[\theta + \sum_{i=1}^{\nu} \phi_i'(w + D) q_i\right] u_{\nu+1} + u_{\nu+2} + (w + D) u_{\nu+3} = 0, \tag{55}$$

$$\begin{aligned}
A_{1i} &= -\theta \phi_i(0) \qquad (i = 1, \ldots, \nu),\\
A_{1\nu+1} &= 1,\\
A_{1\nu+2} &= 0,\\
A_{1\nu+3} &= -\sum_{i=1}^{\nu} \phi_i(0) q_i,
\end{aligned}$$

$$
\begin{aligned}
A_{2i} &= \phi_i(w) \qquad (i = 1, \ldots, \nu),\\
A_{2\nu+1} &= -\theta - \sum_{i=1}^{\nu} \phi_i'(w) q_i,\\
A_{2\nu+2} &= 1,\\
A_{2\nu+3} &= w,\\
A_{3i} &= \phi_i(w + D) \qquad (i = 1, \ldots, \nu),\\
A_{3\nu+1} &= -\theta - \sum_{i=1}^{\nu} \phi_i'(w + D) q_i,\\
A_{3\nu+2} &= 1,\\
A_{3\nu+3} &= w + D,
\end{aligned}
\tag{56}
$$

$$
\begin{aligned}
B_1 &= \dot{w},\\
B_2 &= 0,\\
B_3 &= 0.
\end{aligned}
\tag{57}
$$

As in the formulation of the linearized partial velocities of eqns (17), linearization may not be performed in the development of eqns (56) and (57) prior to the identification of eqns (51) and (52). Premature linearization would result in the loss of terms in $A_{1i}(i = 1, \ldots, \text{m } \nu)$ and $A_{1\nu+3}$.

Since there are three constraints equations, the constrained system has only ν, as opposed to $\nu + 3$, degrees of freedom; hence, only ν independent generalized speeds are needed to describe its motion. If one chooses to regard the first ν generalized speeds $u_i(i = 1, \ldots, \nu)$ as independent, an expression for the remaining three dependent generalized speeds $u_{\nu+1}$, $u_{\nu+2}$, and $u_{\nu+3}$ can be written as

$$
\underline{\hat{u}} = \underline{\alpha}_1 \underline{\tilde{u}} + \underline{\beta}_1, \tag{58}
$$

where $\underline{\hat{u}}$ is a 3×1 matrix of the dependent generalized speeds, $\underline{\tilde{u}}$ is a $\nu \times 1$ matrix of the independent generalized speeds, $\underline{\alpha}_1$ is a $3 \times \nu$ matrix, and $\underline{\beta}_1$ is a 3×1 matrix. After partitioning $\underline{A}$ so that

$$
\underline{A} = [\underline{A}_1 \underline{A}_2], \tag{59}
$$

where $\underline{A}_1$ is $3 \times \nu$ and $\underline{A}_2$ is 3×3, one finds that $\underline{\alpha}_1$ and $\underline{\beta}_1$ are given by

$$
\underline{\alpha}_1 = -\underline{A}_2^{-1} \underline{A}_1, \qquad \underline{\beta}_1 = -\underline{A}_2^{-1} \underline{B}. \tag{60}
$$

The matrices $\underline{A}_1$ and $\underline{A}_2$ can be identified from eqns (56), and the elements of $\underline{\alpha}_1$ are then seen to be

$$
\left.
\begin{aligned}
(\alpha_1)_{1i} &= \theta\phi_i(0) - \frac{1}{D}[\phi_i(w + D) - \phi_i(w)] \sum_{j=1}^{\nu} \phi_j(0) q_j,\\
(\alpha_1)_{2i} &= -\frac{1}{D}[(w - D)\phi_i(w) - w\phi_i(w + D)],\\
(\alpha_1)_{3i} &= -\frac{1}{D}[\phi_i(w + D) - \phi_i(w)],
\end{aligned}
\right\} \qquad (i = 1, \ldots, \nu) \tag{61}
$$

where $\underline{\beta}_1$ is given by

$$\underline{\beta}_1 = -\frac{\dot{w}}{D}\begin{bmatrix} D \\ D\theta + \sum_{i=1}^{\nu}[(w+D)\phi_i'(w) - w\phi_i'(w+D)]q_i \\ \sum_{i=1}^{\nu}[\phi_i'(w+D) - \phi_i'(w)]q_i \end{bmatrix}. \tag{62}$$

In what follows, an expression for $\dot{\underline{u}}$ is needed. This can be written as

$$\dot{\underline{u}} = \underline{\alpha}_1\dot{\underline{u}} + \underline{\delta}_1, \tag{63}$$

where $\underline{\delta}_1$ is the 3×1 matrix defined as

$$\underline{\delta}_1 \triangleq -\underline{A}_2^{-1}(\dot{\underline{A}}\underline{u} + \dot{\underline{B}}). \tag{64}$$

Utilizing eqn (59) and substituting from eqns (56) and (57) into eqn (64), one obtains

$$\begin{aligned}\underline{\delta}_1 = -\frac{1}{D}\Bigg\{ &\ddot{w}\begin{bmatrix} D \\ D\theta + \sum_{i=1}^{\nu}[(w+D)\phi_i'(w) - w\phi_i'(w+D)]q_i \\ \sum_{i=1}^{\nu}[\phi_i'(w+D) - \phi_i'(w)]q_i \end{bmatrix} \\ &+ 2\dot{w}\begin{bmatrix} 0 \\ Du_{\nu+3} + \sum_{i=1}^{\nu}[(w+D)\phi_i'(w) - w\phi_i'(w+D)]u_i \\ \sum_{i=1}^{\nu}[\phi_i'(w+D) - \phi_i'(w)]u_i \end{bmatrix} \\ &+ \dot{w}^2\begin{bmatrix} 0 \\ \sum_{i=1}^{\nu}[(w+D)\phi_i''(w) - w\phi_i''(w+D)]q_i \\ \sum_{i=1}^{\nu}[\phi_i''(w+D) - \phi_i''(w)]q_i \end{bmatrix}\Bigg\}. \end{aligned} \tag{65}$$

Dynamical equations

Before one assembles the dynamical equations which govern the constrained system, it is useful to construct the $(\nu + 3) \times (\nu + 3)$ matrix $\underline{M}$ and the $(\nu + 3) \times 1$ matrix $\underline{N}$ such that

$$\underline{M}\dot{\underline{u}} + \underline{N} = \underline{F}^* + \underline{F} \tag{66}$$

where $\underline{F}^*$ and $\underline{F}$ are $(\nu + 3) \times 1$ matrices whose elements are the generalized inertial forces of eqns (23–26) and the generalized active forces of eqns (29) and (30), respectively. After partitioning $\underline{M}$ and $\underline{N}$ so that

$$\underline{M} = \begin{bmatrix} \underline{M}_{11} & \underline{M}_{12} \\ \underline{M}_{21} & \underline{M}_{22} \end{bmatrix}, \qquad \underline{N} = \begin{bmatrix} \underline{N}_1 \\ \underline{N}_2 \end{bmatrix}, \tag{67}$$

where $\underline{M}_{11}$ is $\nu \times \nu$, $\underline{M}_{12}$ is $\nu \times 3$, $\underline{M}_{21}$ is $3 \times \nu$, $\underline{M}_{22}$ is 3×3, $\underline{N}_1$ is $\nu \times 1$, and $\underline{N}_2$ is 3×1, we use eqns (23–26), (29), and (30) to note that

$$\underline{M}_{11} = \begin{bmatrix} -a_{11} & \dots & -a_{1\nu} \\ \vdots & \vdots & \vdots \\ -a_{\nu 1} & \dots & -a_{\nu\nu} \end{bmatrix},$$

$$\underline{M}_{12} = \begin{bmatrix} \sum_{i=1}^{\nu} b_{i1} q_i + c_1\theta & -c_1 & -d_1 \\ \vdots & \vdots & \vdots \\ \sum_{i=1}^{\nu} b_{i\nu} q_i + c_\nu\theta & -c_\nu & -d_\nu \end{bmatrix},$$

$$\underline{M}_{21} = \begin{bmatrix} 0 & \dots & 0 \\ -c_1 & \dots & -c_\nu \\ -d_1 & \dots & -d_\nu \end{bmatrix}, \tag{68}$$

$$\underline{M}_{22} = \begin{bmatrix} -m & 0 & 0 \\ 0 & -m & -e \\ \sum_{i=1}^{\nu} c_i q_i + e\theta & -e & -J \end{bmatrix},$$

$$\underline{N}_1 = \begin{bmatrix} -\sum_{i=1}^{\nu} h_{i1} q_i \\ \vdots \\ -\sum_{i=1}^{\nu} h_{i\nu} q_i \end{bmatrix}, \qquad \underline{N}_2 = \begin{bmatrix} 0 \\ 0 \\ 0 \end{bmatrix}, \tag{69}$$

and write the constrained dynamical equations as

$$(\underline{M}_{11} + \underline{M}_{12}\underline{\alpha}_1 + \underline{\alpha}_1^{\mathrm{T}}\underline{M}_{21} + \underline{\alpha}_1^{\mathrm{T}}\underline{M}_{22}\underline{\alpha}_1)\dot{\underline{u}} + \underline{N}_1 + \underline{\alpha}_1^{\mathrm{T}}\underline{N}_2 + (\underline{M}_{12} + \underline{\alpha}_1^{\mathrm{T}}\underline{M}_{22})\underline{\delta}_1 = 0, \tag{70}$$

where the superscript "T" denotes the transpose operator.

The scalar equations corresponding to eqn (70), together with the kinematical equations relating $\dot{\underline{u}}$ to $\underline{u}$ [see eqn (58)] and $u_i (i = 1, \dots, \nu + 3)$ to $\dot{q}_i (i = 1, \dots, \nu)$, $\dot{z}_1$, $\dot{z}_2$, and $\dot{\theta}$ [see eqn (5)], form a complete set of equations of motion governing the constrained system. Before the equations can be solved to yield useful results, however, one must specify meaningful initial values for $q_i (i = 1, \dots, \nu)$, z_1, z_2, θ, and $u_i (i = 1, \dots, \nu + 3)$. Concerns that arise in this connection are considered next.

Initial conditions

In general, at the start of a numerical simulation of a motion of B, the points of B have prescribed positions and velocities. To render such prescriptions physically meaningful, one must state them in terms of the variables x, y, and $\dot{y}$, where y is a function of x and t and $\dot{y} \triangleq dy/dt$ (see Fig. 1.). Since the dynamical equations are expressed in terms of the variables $q_i (i = 1, \dots, \nu)$, z_1, z_2, θ, and $u_i (i = 1, \dots, \nu + 3)$, a scheme must be devised to enable one to calculate initial values of the latter when one is given initial values of the former. To develop such a scheme, we begin by considering the

linearized expression for the position vector from $\hat{P}$ to G, which is

$$\mathbf{p}^{\hat{P}G} = (-z_1 + \xi)\mathbf{n}_1 + \left(z_2 + \xi\theta + \sum_{i=1}^{\nu} \phi_i q_i\right)\mathbf{n}_2. \tag{71}$$

This equation is used to express the constraints imposed on the position of H, P, and Q, namely,

$$\mathbf{p}^{\hat{P}H}\cdot\mathbf{n}_1 = -w, \qquad \mathbf{p}^{\hat{P}P}\cdot\mathbf{n}_2 = 0, \qquad \mathbf{p}^{\hat{P}Q}\cdot\mathbf{n}_2 = 0, \tag{72}$$

as

$$z_1 = w, \tag{73}$$

$$z_2 + w\theta + \sum_{i=1}^{\nu} \phi_i(w) q_i = 0, \tag{74}$$

$$z_2 + (w + D)\theta + \sum_{i=1}^{\nu} \phi_i(w + D) q_i = 0. \tag{75}$$

Solving eqns (74) and (75) for z_2 and θ yields

$$z_2 = -\frac{1}{D}\sum_{i=1}^{\nu} [(w + D)\phi_i(w) - w\phi_i(w + D)]q_i, \tag{76}$$

$$\theta = \frac{1}{D}\sum_{i=1}^{\nu} [\phi_i(w) - \phi_i(w + D)]q_i, \tag{77}$$

and substitution from eqns (73), (76), and (77) into eqn (71) then produces

$$\mathbf{p}^{\hat{P}G} = (-w + \xi)\mathbf{n}_1 + \left\{\sum_{i=1}^{\nu} [\phi_i(\xi) - \phi_i(w)]q_i + \frac{1}{D}(\xi - w)\sum_{i=1}^{\nu} [\phi_i(w) - \phi_i(w + D)]q_i\right\}\mathbf{n}_2. \tag{78}$$

This equation is to be employed to determine initial values of $q_i (i = 1, \ldots, \nu)$, z_1, z_2, and θ corresponding to a vector function $\mathbf{p}_o(x)$ describing the initial positions of the points of B relative to $\hat{P}$, where $\mathbf{p}_o(x)$ is given by

$$\mathbf{p}_o(x) = (-w_o + x)\mathbf{n}_1 + y_o(x)\mathbf{n}_2, \tag{79}$$

in which w_o denotes the value of w at $t = 0$ and $y_o(x)$ is a prescribed initial displacement function. Equating $\mathbf{p}_o(x)$ to $\mathbf{p}^{\hat{P}G}$ evaluated at $t = 0$ gives

$$\xi = x, \tag{80}$$

$$z_1(0) = w_o, \tag{81}$$

$$\sum_{i=1}^{\nu} \psi_i(x) q_i(0) = y_o(x), \tag{82}$$

where

$$\psi_i(x) \triangleq \phi_i(x) - \phi_i(w_o) + \frac{1}{D}(x - w_o)[\phi_i(w_o) - \phi_i(w_o + D)] \qquad (i = 1, \ldots, \nu) \tag{83}$$

and $z_1(0)$ and $q_i(0)(i = 1, \ldots, \nu)$ denote the values of z_1 and $q_i(i = 1, \ldots, \nu)$ at $t = 0$. For a specific function $y_o(x)$ and a finite value for ν, there does not exist, in general, any set of $q_i(0)(i = 1, \ldots, \nu)$ such that eqn (82) is satisfied. However, by multiplying both sides of eqn (82) by $\psi_j(x)(j = 1, \ldots, \nu)$ and by integrating from 0 to L, one can determine a set of $q_i(0)$ such that the integral of the square of the difference between the left side of eqn (82) and $y_o(x)$ is minimized. Doing so, expressing the result in a matrix format, gives

$$\underline{K}\,\underline{Q} = \underline{R}, \tag{84}$$

where the elements of the $\nu \times \nu$ matrix $\underline{K}$, the $\nu \times 1$ matrix $\underline{Q}$, and the $\nu \times 1$ matrix $\underline{R}$, are defined, respectively, as

$$K_{ij} \triangleq \int_0^L \psi_i(x)\psi_j(x)\,dx \qquad (i, j = 1, \ldots, \nu), \tag{85}$$

$$Q_i \triangleq q_i(0) \qquad (i = 1, \ldots, \nu), \tag{86}$$

and

$$R_i \triangleq \int_0^L \psi_i(x)y_o(x)\,dx \qquad (i = 1, \ldots, \nu). \tag{87}$$

Thus, by solving eqn (84) for $\underline{Q}$, and by making use of eqns (76) and (77), one obtains values for $q_i(0)(i = 1, \ldots, \nu)$, $z_2(0)$, and $\theta(0)$, where $z_2(0)$ and $\theta(0)$ denote the values of z_2 and θ at $t = 0$, which "best" approximate any prescribed initial displacement function $y_o(x)$.

To determine initial values of $u_i(i = 1, \ldots, \nu + 3)$, one can make use of much of the information developed in connection with determining the initial values of z_1, z_2, θ, and $q_i(i = 1, \ldots, \nu)$. Specifically, one first differentiates eqns (73) and (76–78) with respect to time and obtains

$$u_{\nu+1} = -\dot{w}, \tag{88}$$

$$u_{\nu+2} = -\frac{1}{D}\left\{\sum_{i=1}^{\nu}[(w + D)\phi_i(w) - w\phi_i(w + D)]u_i + \dot{w}\sum_{i=1}^{\nu}[\phi_i(w) - \phi_i(w + D)]q_i + \dot{w}\sum_{i=1}^{\nu}[(w + D)\phi_i'(w) - w\phi_i'(w + D)]q_i\right\}, \tag{89}$$

$$u_{\nu+3} = \frac{1}{D}\left\{\sum_{i=1}^{\nu}[\phi_i(w) - \phi_i(w + D)]u_i + \dot{w}\sum_{i=1}^{\nu}[\phi_i'(w) - \phi_i'(w + D)]q_i\right\}, \tag{90}$$

$$\begin{aligned}\mathbf{v}^G = -\dot{w}\mathbf{n}_1 + \Bigg\{&\sum_{i=1}^{\nu}[\phi_i(\xi) - \phi_i(w)]u_i + \frac{1}{D}(\xi - w)\sum_{i=1}^{\nu}[\phi_i(w) - \phi_i(w + D)]u_i \\ &- \dot{w}\sum_{i=1}^{\nu}\phi_i'(w)q_i - \frac{\dot{w}}{D}\sum_{i=1}^{\nu}[\phi_i(w) - \phi_i(w + D)]q_i \\ &+ \frac{\dot{w}}{D}(\xi - w)\sum_{i=1}^{\nu}[\phi_i'(w) - \phi_i'(w + D)]q_i\Bigg\}\mathbf{n}_2,\end{aligned} \tag{91}$$

where $\mathbf{v}^G$ is the velocity of G. Next, whenever a function $\mathbf{v}_o(x)$ describing the initial velocities of the points of B can be written as

$$\mathbf{v}_o(x) = -\dot{w}_o\mathbf{n}_1 + \dot{y}_o(x)\mathbf{n}_2, \tag{92}$$

where $\dot{w}_o$ denotes the value of $\dot{w}$ at $t = 0$ and $\dot{y}_o(x)$ denotes a prescribed initial motion function, one takes steps analogous to those used to develop eqn (84) to obtain the

matrix equation

$$\underline{K}\,\underline{U} = \underline{S}\,\underline{Q} + \underline{T}, \tag{93}$$

where the $\nu \times \nu$ matrix $\underline{K}$ and the $\nu \times 1$ matrix $\underline{Q}$ are identical to those in eqn (84), and the elements of the $\nu \times 1$ matrix $\underline{U}$, the $\nu \times \nu$ matrix $\underline{S}$, and the $\nu \times 1$ matrix $\underline{T}$ are defined, respectively, as

$$U_i \triangleq u_i(0) \qquad (i = 1, \ldots, \nu), \tag{94}$$

$$S_{ij} \triangleq \dot{w}_o \int_0^L \Xi_i(x)\psi_j(x)\,dx \qquad (i, j = 1, \ldots, \nu), \tag{95}$$

$$T_i \triangleq \int_0^L \psi_i(x)\dot{y}_o(x)\,dx \qquad (i = 1, \ldots, \nu), \tag{96}$$

where

$$\Xi_i(x) \triangleq \phi_i'(w_o) + \frac{1}{D}[\phi_i(w_o) - \phi_i(w_o + D)] - \frac{1}{D}(x - w_o)[\phi_i'(w_o) - \phi_i'(w_o + D)] \qquad (i = 1, \ldots, \nu). \tag{97}$$

Once eqn (84) has been solved for $q_i(0)(i = 1, \ldots, \nu)$, eqn (93) can be solved for $u_i(0)(i = 1, \ldots, \nu)$. The initial values of $u_{\nu+1}$, $u_{\nu+2}$, and $u_{\nu+3}$ then are obtained from eqns (88–90).

Solution algorithm

The preceding analysis shows that one can proceed as follows to perform numerical simulations of motions of B:

(1) Specify values for the parameters D, ρ, L, and EI, and calculate the constants m, e, and J as defined by eqns (21).
(2) Specify a value for ν; select modal functions $\phi_i(\xi)(i = 1, \ldots, \nu)$; refer to eqns (22) to evaluate the constants a_{ij}, b_{ij}, c_i, and $d_i(i, j = 1, \ldots, \nu)$; and use eqn (31) to determine $h_{ij}(i, j = 1, \ldots, \nu)$.
(3) Specify the function $w(t)$.
(4) Specify the initial displacement function $y_o(x)$ and the initial motion function $\dot{y}_o(x)$, and calculate $q_i(0)(i = 1, \ldots, \nu)$, $z_1(0)$, $z_2(0)$, $\theta(0)$, and $u_i(0)(i = 1, \ldots, \nu + 3)$ using eqns (76), (77), (81), (84), (88–90), and (93).
(5) At each step of a simulation:
  (a) Construct the matrices $\underline{\alpha}_1$ and $\underline{\beta}_1$ of eqns (61) and (62).
  (b) Construct expressions for $u_{\nu+1}$, $u_{\nu+2}$, and $u_{\nu+3}$ using eqn (58).
  (c) Construct the matrix $\underline{\delta}_1$ of eqn (65).
  (d) Construct the matrices $\underline{M}_{11}$, $\underline{M}_{12}$, $\underline{M}_{21}$, $\underline{M}_{22}$, $\underline{N}_1$, and $\underline{N}_2$ of eqns (68) and (69).
  (e) Construct the dynamical equations as given in eqn (70).
  (f) Assemble $2\nu + 3$ first-order differential equations for the time-derivatives of the $2\nu + 3$ variables $q_i(i = 1, \ldots, \nu)$, z_1, z_2, θ, and $u_i(i = 1, \ldots, \nu)$ from eqns (5) and eqn (70).
(6) Substitute values of the q_i and $u_i(i = 1, \ldots, \nu)$ obtained by solving eqns (5) and (70) into eqns (78) and (91) to gain physically relevant information regarding the positions and velocities of points of B.

SIMULATIONS

The equations generated in the preceding section have been incorporated into a numerical simulation program used in this section to investigate the response of B in three situations: when B undergoes no longitudinal motion, when B undergoes sinu

soidal longitudinal motion, and when B undergoes longitudinal motion for the purpose of repositioning.

No longitudinal motion

When the longitudinal displacement function w is equal to a constant, the beam B can perform only transverse motions, and functions describing these motions can be obtained by classical methods. These functions can be used to test the present formulation, as follows:

(1) The first step of the solution algorithm is the specification of values for the distance D between support points and for the beam's mass per unit length ρ, total length L, and flexural stiffness EI. We take

$$D = 0.25 \text{ m}, \quad \rho = 1.0 \text{ kg/m}, \quad L = 1.0 \text{ m}, \quad EI = 1.0 \text{ N-m}^2. \tag{98}$$

The definitions of m, e, and J given in eqns (21) are incorporated directly into the program, so the evaluation of these constants is left to the computer.

(2) Modal functions $\phi_i (i = 1, \ldots, \nu)$ may be chosen arbitrarily so long as the boundary conditions of B are satisfied; however, two concerns one should keep in mind are physical realism and analytical convenience. These concerns are addressed in the Elaborative Comments section of this article; for the moment, we let

$$\phi_i(\xi) \triangleq \cos\left(\frac{\lambda_i \xi}{L}\right) + \cosh\left(\frac{\lambda_i \xi}{L}\right) - \gamma_i \left[\sin\left(\frac{\lambda_i \xi}{L}\right) + \sinh\left(\frac{\lambda_i \xi}{L}\right)\right] \quad (i = 1, \ldots, \nu), \tag{99}$$

where

$$\gamma_i \triangleq \frac{\cos \lambda_i - \cosh \lambda_i}{\sin \lambda_i - \sinh \lambda_i} \qquad (i = 1, \ldots, \nu), \tag{100}$$

and $\lambda_1, \ldots, \lambda_\nu$ are the consecutive roots of the transcendental equation

$$1 - \cos \lambda \cosh \lambda = 0. \tag{101}$$

The modal functions defined in eqn (99) are obtained from the classical theory governing transverse vibrations of a uniform, unrestrained beam[1]. For the ensuing numerical simulations, the number of modes ν is taken to be in the range from one to nine, and the evaluation of the constants a_{ij}, b_{ij}, c_i, d_i, and $h_{ij} (i, j = 1, \ldots, \nu)$ of eqns (22) and (31) is performed by the computer. In programming the expressions that define these constants, advantage is taken of properties of $\phi_i (i = 1, \ldots, \nu)$ which allow one to write

$$\left.\begin{aligned} a_{ij} &= m\delta_{ij}, \\ b_{ij} &= \rho \begin{cases} \dfrac{\lambda_i \gamma_i}{2}(\lambda_i \gamma_i + 6) & (i = j), \\ \dfrac{4}{(\lambda_i^4 - \lambda_j^4)^2}[(\lambda_i^4 - \lambda_j^4)(\lambda_i^4 \lambda_j \gamma_j - \lambda_i \lambda_j^4 \gamma_i) & \\ \qquad + 8\lambda_i^4 \lambda_j^4] & (i \neq j;\ i + j \text{ odd}), \\ \dfrac{4}{(\lambda_i^4 - \lambda_j^4)}(\lambda_i^4 \lambda_j \gamma_j & \\ \qquad - \lambda_i \lambda_j^4 \gamma_i) & (i \neq j;\ i + j \text{ even}), \end{cases} \\ c_i &= d_i = 0, \\ h_{ij} &= EI \frac{\lambda_i^4}{L^3} \delta_{ij}, \end{aligned}\right\} \quad (i, j = 1, \ldots, \nu) \tag{102}$$

where δ_{ij} is the Kronecker delta.

(3) The function w is taken to be

$$w = 0.375 \text{ m}. \tag{103}$$

Referring both to Fig. 1 and to the values of D and L given in eqns (98), one can observe that, as a result of this choice for w, B is centered over a point midway between the supports $\hat{P}$ and $\hat{Q}$.

(4) To compare numerical values produced by using the present formulation with those corresponding to the classical theory, B is taken to be initially at rest and deformed into the first flexural mode of free vibration, with the perpendicular distance from line N_1 to point H equal to 0.01 m. Accordingly, the initial displacement function y_o (in meters) and the initial motion function $\dot{y}_o$ appearing in eqns (79) and (92), respectively, are

$$y_o = 0.005 \begin{cases} \cos\left(\frac{\alpha x_1}{L}\right) + \cosh\left(\frac{\alpha x_1}{L}\right) \\ \quad - 0.772\left[\sin\left(\frac{\alpha x_1}{L}\right) + \sinh\left(\frac{\alpha x_1}{L}\right)\right] (0.0 \le x \le 0.375), \\ -0.712\left[\cos\left(\frac{\alpha x_2}{L}\right) - \cosh\left(\frac{\alpha x_2}{L}\right)\right] \\ \quad - 0.362\left[\sin\left(\frac{\alpha x_2}{L}\right) + \sinh\left(\frac{\alpha x_2}{L}\right)\right] \\ \quad - 0.031\left[\sin\left(\frac{\alpha x_2}{L}\right) - \sinh\left(\frac{\alpha x_2}{L}\right)\right] (0.375 < x \le 0.625), \\ -0.712\left[\cos\left(\frac{\alpha x_3}{L}\right) - \cosh\left(\frac{\alpha x_3}{L}\right)\right] \\ \quad + 0.362\left[\sin\left(\frac{\alpha x_3}{L}\right) + \sinh\left(\frac{\alpha x_3}{L}\right)\right] \\ \quad + 0.682\left[\sin\left(\frac{\alpha x_3}{L}\right) - \sinh\left(\frac{\alpha x_3}{L}\right)\right] (0.625 < x \le 1.0). \end{cases} \tag{104}$$

and

$$\dot{y} = 0, \tag{105}$$

where $x_1 = x$, $x_2 = x - 0.375$, $x_3 = x - 0.625$, and $\alpha = 4.031$. The values of $q_i(0)(i = 1, \ldots, \nu)$, $z_1(0)$, $z_2(0)$, $\theta(0)$, and $u_i(0)(i = 1, \ldots, \nu + 3)$ are computed by using the equations listed in the solution algorithm.

(5) The construction of the dynamical equations governing motions of B is relegated to the computer and proceeds as specified in the solution algorithm.

(6) Values of q_i and $u_i(i = 1, \ldots, \nu)$ generated by numerical integrating eqns (5) and (70) are substituted into eqns (78) and (91) to obtain information about the positions and velocities of points of B.

Figure 5 shows a plot of the transverse displacement of point H versus time for $w = 0.375$. The solid line represents the classical solution, and the black squares correspond to values obtained using the current formulation with $\nu = 3$. The two solutions are seen to be in complete agreement. Additional information is provided in Table 1, where frequencies of free vibrations obtained both by classical methods and by solving eqns (70) are reported for $\nu = 1$, 2, 3, 5, and 9. As can be observed, for $\nu = 1$, the value of the first natural frequency is in excellent agreement (less than 1% error) with the value predicted by classical theory; for $\nu = 5$, the first three frequencies are in excellent agreement; and for $\nu = 9$, all nine frequencies agree very well. These

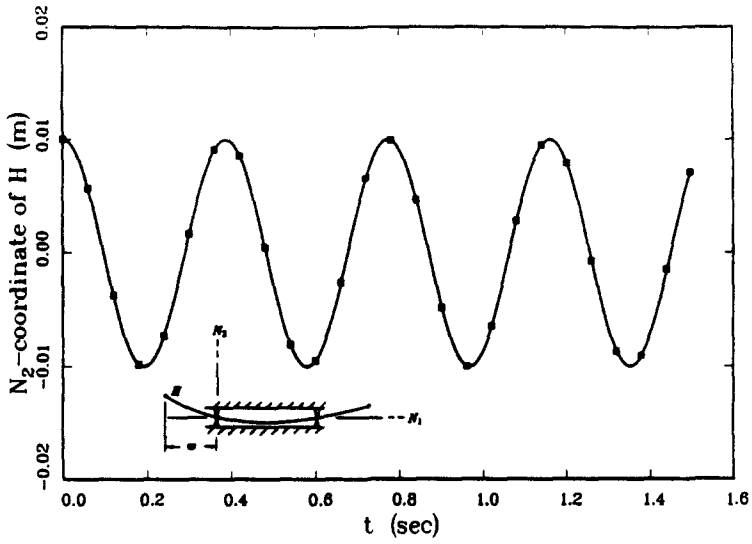

Fig. 5. No longitudinal motion with $w = 0.375$ m.

results, which are important in connection with upcoming instability considerations, show that the present approach to solving the problem of a beam moving over supports correctly predicts the natural frequencies of a beam that is fixed longitudinally.

Sinusoidal longitudinal motions

Consider next a situation in which B moves longitudinally over its supports with a motion that varies sinusoidally with time. In generating the response of B to this type of excitation, one can utilize many of the same data used previously. Specifically, the same system parameters as in eqn (98) and the same modal functions as in eqn (99) apply. The initial displacement function (in meters) and motion function are now

$$y_o = \begin{Bmatrix} E_2x_1^4 + E_3x_1 + E_4 & (x \le w_o), \\ E_2x_2^4 + E_5x_2^3 + E_6x_2^2 + E_7x_2 & (w_o < x \le w_o + D), \\ E_2x_3^4 + E_8x_3^3 + E_9x_3^2 + E_{10}x_3 & (w_o + D < x \le L), \end{Bmatrix} \tag{106}$$

and

$$\dot{y}_o = 0, \tag{107}$$

where

$$\begin{aligned} E_1 &= 2(L - w_o - D)^2 - D^2 + 4w_o^2, \\ E_2 &= 0.01/(3w_o^4 + w_oDE_1), \\ E_3 &= -E_2(4w_o^3 + DE_1), \\ E_4 &= w_oE_2(3w_o^3 + DE_1), \\ E_5 &= 2E_2[(L - w_o - D)^2 - D^2 - w_o^2]/D, \\ E_6 &= 6w_o^2E_2, \\ E_7 &= -DE_2[2(L - w_o - D)^2 - D^2 + 4w_o^2], \\ E_8 &= -4E_2(L - w_o - D), \\ E_9 &= 6E_2(L - w_o - D)^2, \\ E_{10} &= DE_2[4(L - w_o - D)^2 - D^2 + 2w_o^2], \end{aligned} \tag{108}$$

Table 1. Frequencies of free vibration in rad/s for $w = 0.375$ m.

Mode No.	Classical Solution	Assumed Modes Solution $\nu = 1$	$\nu = 2$	$\nu = 3$	$\nu = 5$	$\nu = 9$
1	16.246	16.268	16.268	16.262	16.255	16.247
2	20.771	—	22.051	22.051	20.906	20.825
3	117.93	—	—	118.29	118.13	117.95
4	136.07	—	—	—	138.38	136.95
5	247.47	—	—	—	260.97	248.85
6	386.11	—	—	—	—	388.79
7	422.58	—	—	—	—	427.03
8	702.44	—	—	—	—	707.16
9	799.47	—	—	—	—	807.16

and $x = x_1$, $x_2 = x - w_o$, $x_3 = x - w_o - D$, and w_o denotes the initial value of w. The initial shape prescribed by y_o corresponds to that which B would take if deformed by a statically applied, uniform load such that the distance from N_1 to H is 0.01 meters. Two expressions are used for the longitudinal displacement function w. These are

$$w = 0.375 - 0.05 \sin 10.0t \text{ m}, \tag{109}$$

and

$$w = 0.375 - 0.05 \sin 20.0t \text{ m}. \tag{110}$$

Both give rise to longitudinal oscillations of the midpoint of B about a point centered between $\hat{P}$ and $\hat{Q}$. The only difference between the two expressions is that they involve different frequencies of oscillation.

Figure 2, discussed briefly in the Introduction, shows the predicted transverse displacement of point H when B is displaced longitudinally in accordance with eqn (109) and when $\nu = 4$. As can be observed, the response is not harmonic but is otherwise unremarkable. Figure 3 displays the transverse displacement of H when w is given by eqn (110) and $\nu = 4$. Clearly, the responses depicted in Figs. 2 and 3 are radically different, and one can see that B may respond to a sinusoidal longitudinal motion in at least two ways, one of which may be characterized as "stable" (Fig. 2) and the other as "unstable" (Fig. 3). The question of instability is pursued further under the heading Instability of Periodic Motions.

Repositional longitudinal motions

A repositional longitudinal motion is one such that B starts from rest in a specified longitudinal position and then is brought to rest in a new longitudinal position. The functional form of w used to generate this type of motion is

$$w = C_1 - \frac{C_2}{T}\left[t - \frac{T}{2\pi}\sin\left(\frac{2\pi t}{T}\right)\right] \text{ m}, \tag{111}$$

where C_1 specifies the initial position of the beam, C_2 is the distance traversed by B, and T is the duration of the maneuver.

Figure 6 displays the predicted transverse displacement of point H (with $\nu = 5$) for $0 \leq t \leq 3.5$ sec when C_1, C_2, and T have the values 0.725 m, 0.70 m, and 3.5 sec, respectively. The notable aspects of this figure are that both the amplitude and the period of oscillation decrease during the motion. Figure 7 again shows the transverse displacement of H during a repositioning maneuver, but now the response is generated with C_1, C_2, and T equal to 0.725 m, 0.70 m, and 0.70 sec, respectively. In other words, Fig. 7 corresponds to repositioning B five times as rapidly as in Fig. 6. While the ultimate result of the two repositioning maneuvers is essentially the same, the amplitude of the transverse displacement of H increases initially in Fig. 7, whereas it decreases in Fig.

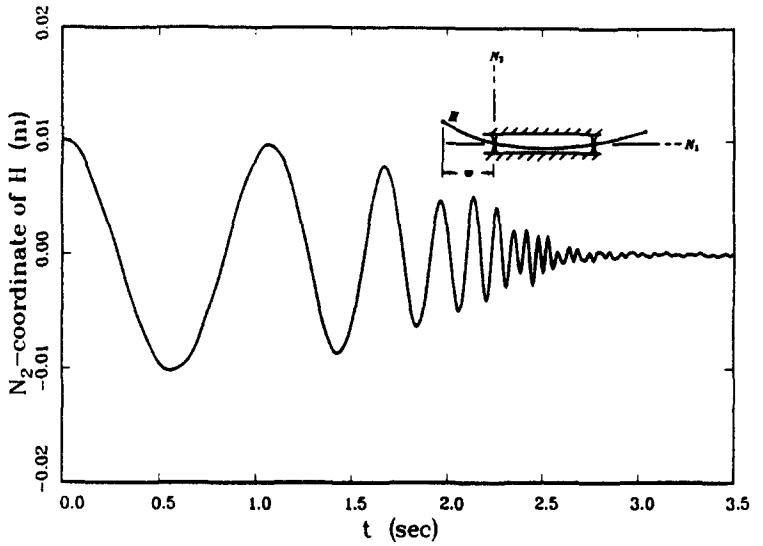

Fig. 6. Slow repositional maneuver with $C_1 = 0.725$ m, $C_2 = 0.70$ m, and $T = 3.5$ sec.

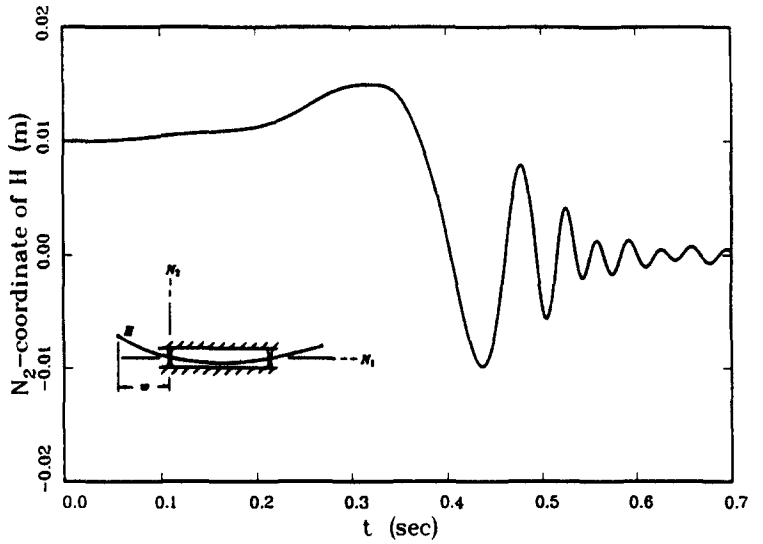

Fig. 7. Rapid repositional maneuver with $C_1 = 0.725$ m, $C_2 = 0.70$ m, and $T = 0.70$ sec.

6. To understand this, one may note that *longitudinal* motions give rise to *transverse* inertia forces that grow in magnitude as longitudinal acceleration increases. The following observations are of interest in this connection: It can be shown that the effect under consideration is associated with the appearance in eqn (70) of $b_{ij}(i, j = 1, \ldots, \nu)$. Reference to eqn (22) shows that the b_{ij} depend on $\epsilon_{ij}(i, j = 1, \ldots, \nu)$, and ϵ_{ij} appear when the partial velocities of eqns (12) are formed using *nonlinear* kinematical expressions. The differences between Figs. 6 and 7 thus demonstrate the importance of adhering strictly to the dictates of Kane's method, one of which is that one must start with *nonlinear kinematical* equations in developing *linear dynamical* equations.

Before examining one final repositional maneuver, recall that for both Figs. 6 and 7, the longitudinal motion of B is in the $\mathbf{n}_1$ direction (see Fig. 4), and the beam is thus being pushed, rather than pulled, over the supports. Figure 8 corresponds to pulling B over its supports, this figure being obtained when C_1, C_2, and T of eqn (111) are equal to 0.025 m, -0.70 m, and 0.70 sec, respectively. Even though the maneuver is performed as quickly as that of Fig. 7, the deflection of the endpoint of B moving toward the supports, in this case the endpoint E, now does not increase initially but decreases quite rapidly. This shows that inertial forces can cause the deflection of an endpoint of B either to increase or decrease.

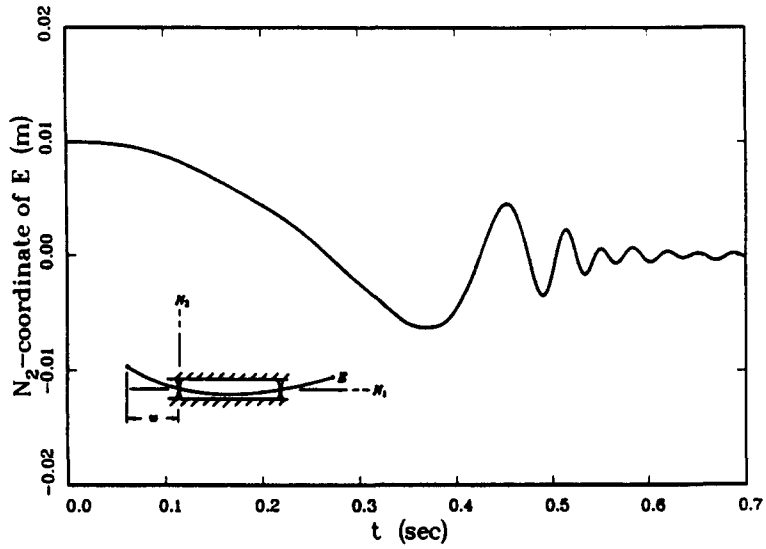

Fig. 8. Rapid reverse repositional maneuver with $C_1 = 0.025$ m, $C_2 = -0.70$ m, and $T = 0.70$ sec.

INSTABILITY OF PERIODIC MOTION

As has been shown, longitudinal displacements of an endpoint of B that vary sinusoidally with time can induce either "stable" or "unstable" transverse motions of B. In this section, methods are presented for predicting whether or not a given periodic longitudinal displacement will give rise to an unstable response. This development is achieved by utilizing results obtained by Floquet, as presented in [5], and by Hsu in [6].

Floquet's theory

A complete treatment of Floquet's theory is available in [5]; however, some of the basic elements of the theory are reviewed here to provide a point of departure for subsequent discussions.

Floquet's theory yields information about the character of the null solution for a system of n first-order, linear, ordinary differential equations with periodic coefficients. When these equations are expressed as

$$\frac{d\underline{X}}{dt} = \underline{\Gamma}\,\underline{X}, \tag{112}$$

where $\underline{X}$ is an $n \times 1$ matrix of dependent variables, and Γ is an $n \times n$ matrix of continuous periodic functions of t with period τ, their solution can be expressed as a sum of $n \times 1$ matrix functions $\underline{\Lambda}_i(t)(i = 1, \ldots, n)$ multiplied by exponential functions $e^{\rho_i t}(i = 1, \ldots, n)$; that is,

$$\underline{X} = \sum_{i=1}^{n} \underline{\Lambda}_i e^{\rho_i t}, \tag{113}$$

where ρ_i are given by

$$\rho_i = \frac{1}{\tau}(\ln |\zeta_i| + \sqrt{-1}\arg \zeta_i) \qquad (i = 1, \ldots, n), \tag{114}$$

and $\zeta_i(i = 1, \ldots, n)$ are the eigenvalues of the $n \times n$ matrix $\underline{Y}(\tau)$, $\underline{Y}(t)$ satisfying the differential equation

$$\frac{d\underline{Y}}{dt} = \underline{\Gamma}\,\underline{Y}, \tag{115}$$

and the initial condition $\underline{Y}(0) = \underline{I}$, where $\underline{I}$ is the $n \times n$ identity matrix.

Instability information is obtained by noting that $\underline{X}$ grows exponentially (i.e., the solution $\underline{X} = 0$ is unstable) whenever one or more of $|\zeta_i| (i = 1, \ldots, n)$ exceeds unity. In general, one must resort to numerical techniques to evaluate ζ_i; that is, by numerically integrating eqn (115) from $t = 0$ to $t = \tau$, with $\underline{Y}(0)$ equal to the identity matrix, one can calculate $\zeta_i (i = 1, \ldots, n)$. Note that without a precise knowledge of the functional form of the $\underline{\Lambda}_i (i = 1, \ldots, n)$, one can guarantee only that values of $|\zeta_i|$ greater than unity imply instability, but not that values of $|\zeta_i|$ less than unity guarantee stability.

To apply Floquet's theory to the analysis of periodic longitudinal motions of B, one first must express the governing equations in the form of eqn (112). This can be accomplished with any general set of modal functions $\phi_i (i = 1, \ldots, \nu)$; however, here the ϕ_i of eqn (99) are used. After taking n equal to 2ν and defining $\underline{X}$ to be the $2\nu \times 1$ matrix

$$\underline{X} \triangleq \begin{bmatrix} u_1 \\ \vdots \\ u_\nu \\ q_1 \\ \vdots \\ q_\nu \end{bmatrix}, \tag{116}$$

one can write the $2\nu \times 2\nu$ matrix $\underline{\Gamma}$ in partitioned form as

$$\underline{\Gamma} = \begin{bmatrix} -\underline{\Delta}_1^{-1}\underline{\Delta}_2 & -\underline{\Delta}_1^{-1}\underline{\Delta}_3 \\ \underline{I} & \underline{0} \end{bmatrix}, \tag{117}$$

where typical elements of the $\nu \times \nu$ matrices $\underline{\Delta}_1$, $\underline{\Delta}_2$, and $\underline{\Delta}_3$ are developed from eqn (70) and expressed as

$$\begin{aligned}
(\Delta_1)_{ij} &= \mu_{ij} + m\delta_{ij}, \\
(\Delta_2)_{ij} &= \frac{2\dot{w}}{D^2}[(m\kappa_i + e\chi_i)(\pi_j - \chi_j) + (e\kappa_i + J\chi_i)\chi_j'], \\
(\Delta_3)_{ij} &= \frac{\ddot{w}}{D^2}\{[mD\phi_i(0) + e\chi_i]\chi_j + mD\chi_i\phi_j(0) \\
&\quad + (m\kappa_i + e\chi_i)(\pi_j - \chi_j) + (e\kappa_i + J\chi_i)\chi_j' \qquad (i, j = 1, \ldots, \nu) \\
&\quad + D^2 b_{ij}\} + \frac{\dot{w}^2}{D^2}[(m\kappa_i + e\chi_i)(\tau_j - 2\chi_j') \\
&\quad + (e\kappa_i + J\chi_i)\chi_j''] + \frac{EI}{L^3}\lambda_i^4\delta_{ij},
\end{aligned} \tag{118}$$

where

$$\begin{aligned}
\kappa_i(w) &\triangleq (w + D)\phi_i(w) - w\phi_i(w + D), \\
\chi_i(w) &\triangleq \phi_i(w + D) - \phi_i(w), \\
\pi_i(w) &\triangleq (w + D)\phi_i'(w) - w\phi_i'(w + D), \qquad (i, j = 1, \ldots, \nu) \\
\tau_i(w) &\triangleq (w + D)\phi_i''(w) - w\phi_i''(w + D), \\
\mu_{ij}(w) &\triangleq \frac{1}{D^2}[\kappa_i(m\kappa_j + e\chi_j) + \chi_i(e\kappa_j + J\chi_j)],
\end{aligned} \tag{119}$$

and $\underline{I}$ and $\underline{0}$ are $\nu \times \nu$ identity and zero matrices, respectively.

Equation (117) has been incorporated into a computer program for the numerical integration of eqn (115). While this program is applicable to the study of any periodic longitudinal motion of B, the present investigation is restricted to harmonic longitudinal motion. Consequently, we take

$$w = w^* - A \sin \Omega t, \tag{120}$$

where w^* is the value of w which specifies the position about which B oscillates, and A and Ω are constants. The following input data must be specified in order to execute the program: the system parameters D, ρ, L, and EI; the number of modal functions ν; and the parameters w^*, A, and Ω. The program then sets $\underline{Y}(0) = \underline{I}$, the $2\nu \times 2\nu$ identity matrix, integrates eqn (115) from $t = 0$ to $t = 2\pi/\Omega$, and determines the eigenvalues $\zeta_i (i = 1, \ldots, 2\nu)$ of the matrix $\underline{Y}(\tau)$.

Figure 9 is an instability chart constructed with the aid of the program just described. The system parameters chosen for this investigation are the same as those in eqn (98), while $\nu = 2$ and $w^* = 0.375$ m, giving rise to oscillatory motions about the position that B occupies when centered over its supports. The amplitude A and frequency Ω of the longitudinal oscillations are assigned values varying discretely from 0.002 m to 0.05 m by 0.002 m, in the case of A, and from 2.0 rad/s to 50.0 rad/s by 2.0 rad/s, for Ω. Each "X" shown on the chart represents an A-Ω pair which leads to values for $\zeta_i (i = 1, \ldots, 2\nu)$ such that at least one has an absolute value greater than unity. The physical significance of Fig. 9 becomes apparent in the light of Figs. 2 and 3, both of which apply when $A = 0.05$ m; but $\Omega = 10.0$ rad/s for Fig. 2, and $\Omega = 20.0$ rad/s for Fig. 3. Hence, Figs 2 and 3 are represented in Fig. 9 by the two squares located at positions corresponding to $A = 0.05$ m and $\Omega = 10.0$ rad/s, and $A = 0.05$ m and $\Omega = 20.0$ rad/s. The fact that the first of these is empty, whereas the second contains a "X", means that Fig. 9 is, in effect, predicting the qualitative difference between Figs. 2 and 3.

Hsu's determinations

Additional instability information can be obtained by using a method developed by Hsu[6], who employs perturbation techniques to locate regions of instability for a general system of m linear, second-order, ordinary differential equations of the form

$$\frac{d^2\underline{Z}}{dt^2} + \epsilon \underline{P}(t) \frac{d\underline{Z}}{dt} + [\underline{\omega} + \epsilon \underline{Q}(t)]\underline{Z} = \underline{0}, \tag{121}$$

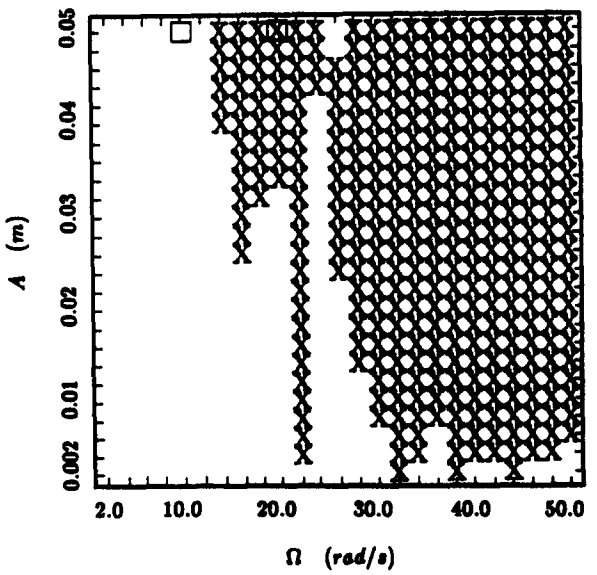

Fig. 9. Instability chart with $w = 0.375 - A \sin \Omega t$ m.

where $\underline{Z}$ is an $m \times 1$ matrix of dependent variables, $\underline{P}(t)$ and $\underline{Q}(t)$ are periodic $m \times m$ matrices of period τ, $\underline{\omega}$ is an $m \times m$ diagonal matrix with elements $\omega_i^2 (i = 1, \ldots, m)$, and ϵ is a small parameter. As in the numerical procedure based on Floquet's theory, Hsu's determinations can be applied to any periodic longitudinal motion of B. For the study at hand, attention is confined to motions of B such that w is of the form of eqn (120). After eqns (5) and (70) are expressed in the form of eqn (121), where again advantage is taken of the modal functions of eqn (99) and where the amplitude A of longitudinal oscillation [see eqn (120)] plays the role of ϵ, Hsu's method enables one to conclude that, for small values of A, regions of instability are centered about values for the frequency of oscillation Ω given by

$$\Omega = \omega_i + \omega_j \qquad (i, j = 1, \ldots, \nu), \tag{122}$$

and/or

$$\Omega = \omega_j - \omega_i \qquad (i, j = 1, \ldots, \nu; i < j), \tag{123}$$

where ω_i and $\omega_j (i, j = 1, \ldots, \nu)$ are the first ν frequencies of transverse vibration for a longitudinally fixed beam whose location is defined by eqn (120) with $A = 0$. The conditions under which eqn (122) and/or eqn (123) are applicable are specified in [6]. For the values of D, ρ, L, EI, w^*, and ν used in generating the instability chart of Fig. 9, one can show that Hsu's determinations indicate that the values of Ω given in eqn (122) give rise to unstable motions of B while those of eqn (123) do not. Recalling the results presented in Table 1 for $\nu = 2$, one finds that the regions of instability depicted in Fig. 9 should be centered, therefore, about the frequencies 32.536, 38.319, and 44.101 rad/s for small values of A. Inspection of Fig. 9 reveals that the regions of instability taper as A decreases and that only frequencies of 32, 38, and 44 rad/s produce unstable points at $A = 0.002$ meters, precisely as eqn (122) predicts.

Observations

Hsu refers to the frequencies of instability predicted by eqns (122) and (123) as "instability frequencies of the first approximation." This terminology stems from using only the first term of a perturbation series to obtain his results. He suggests that additional frequencies of instability exist but that a one term series does not indicate them explicitly. In the light of well-known results for a single second order ordinary differential equation with poeriodic coefficients, such as Mathieu's equation, the system depicted in Fig. 1 may be expected to possess additional values of Ω about which regions of instability are centered, these values being

$$\Omega = \frac{\omega_i + \omega_j}{k} \qquad (i, j = 1, \ldots, \nu; k = 2, \ldots, \infty), \tag{124}$$

and/or

$$\Omega = \frac{\omega_j - \omega_i}{k} \qquad (i, j = 1, \ldots, \nu; i < j; k = 2, \ldots, \infty), \tag{125}$$

where ω_i and ω_j are again frequencies of free vibration for a longitudinally fixed beam. For the system parameters leading to Fig. 9, only eqn (124) applies, and numerical values for the additional instability frequencies are 22.051, 19.159, and 16.268 rad/s, for $k = 2$, 14.700, 12.773, and 10.845 rad/s, for $k = 3$, etc. By returning to Fig. 9, one can see that narrow regions of instability do, indeed, extend toward the line of zero amplitude at $\Omega = 16$ and $\Omega = 22$ rad/s. Additionally, though not apparent in Fig. 9, narrow instability regions have been found centered about the remaining frequency values given in eqn (124) for $k = 2, 3$.

Equations (124) and (125) indicates that many more regions of instability exist than are identified by eqns (122) and (123). The majority of the additional regions identified

by eqn (124) do not make significant contributions to the instability chart of Fig. 9 for several reasons. First, the chart of Fig. 9 only applies to discrete values A and Ω; hence, unstable regions lying entirely between values investigated are lost. Second, results reported both by Hsu and by Meirovitch[12] suggest that the width of a region of instability associated with a frequency $(\omega_i + \omega_j)/k$ is proportional to A^k for small values of A. Therefore, instability regions predicted with $k = 1$ grow linearly with A, those predicted with $k = 2$ grow parabolically, those with $k = 3$ grow cubically, etc. and regions corresponding to large values of k are vanishingly thin for $A \ll 1$. Finally, the instability regions associated with large values of k are not only vanishingly thin, but also are incalculably weak for small A. That is, even if one could determine *a priori* an A-Ω pair corresponding to an unstable region associated with a large value of k, the resulting values for the eigenvalues $\zeta_i (i = 1, \ldots, 2\nu)$ [see eqn (114)], for small A, would be numerically indistinguishable from unity and would not reliably reflect the presence of an unstable region.

While the above statements identify limitations of the numerical procedure employed in producing Fig. 9, these limitations are not serius. On the basis of experiments, Hsu proposes that instability regions associated with small values of k are the most important. He indicates that damping, present at least to a small extent in actual systems, overpowers the weak regions of instability associated with large values of k. Consequently, regions of instability not contributing to Fig. 9 are those regions least important in predicting the behavior of any real system.

Instability conclusions

The conclusions to be drawn from the foregoing are twofold. First, for "small", harmonic, longitudinal oscillations of a beam moving over supports, regions of instability are centered about the frequencies $\omega_i + \omega_j (i, j = 1, \ldots, \nu)$ and/or $\omega_j - \omega_i (i, j = 1, \ldots, \nu;\ i < j)$, where ω_i and ω_j are frequencies of transverse vibration for a corresponding longitudinally fixed beam. Based on the evidence presented above, less significant instability regions also exist at the frequencies $(\omega_i + \omega_j)/k (i, j = 1, \ldots, \nu;\ k = 2, \ldots, \infty)$ and/or $(\omega_j - \omega_i)/k (i, j = 1, \ldots, \nu;\ i < j;\ k = 2, \ldots, \infty)$. Second, accurate instability information can be obtained for *any* amplitude of periodic motion by utiizing the presented numerical procedure. As opposed to potentially lengthy numerical simulations, this procedure allows one to produce definitive instability predictions on the basis of a numerical integration of the governing equations over only a single period of motion. Moreover, when the procedure is used in conjunction with a knowledge of the location of regions of instability for small amplitudes of oscillation, one can ensure that all significant regions are accounted for.

Corroborative results are obtained by Barr[13] for the special case of harmonic longitudinal motions of a cantilever beam. {Harmonic longitudinal motions of B approach those of a cantilever beam when w^* [see eqn (120)] and D (see Fig. 1) both approach zero.} He predicts that regions of instability are centered, for small amplitudes of motion, about the frequencies $\bar{\omega}_i + \bar{\omega}_j (i, j = 1, \ldots, \bar{\nu})$, where the $\bar{\omega}_i (i = 1, \ldots, \bar{\nu})$ are natural frequencies for a fixed cantilever beam, and $\bar{\nu}$ is the number of modal functions used in the analysis. Moreover, Barr reports that experiments performed by sinusoidally driving a cantilever strip through a slot confirm his predictions.

Finally, it is worth noting that, for the sake of economy in generating Fig. 9, all data were calculated with $\nu = 2$. The consequence of utilizing larger values for ν is a slight shift to the left of the instability regions exhibited. This shift reflects small changes in ω_1 and ω_2 resulting from improved approximations to their actual values obtainable by using more modes (see Table 1).

ELABORATIVE COMMENTS

Three concerns deserving additional consideration have been identified in the preceding sections. The first arises from the fact that the equations of motion are formulated by regarding the beam as unrestrained at the outset of the analysis. The second is that the choice of modal functions is largely arbitrary. The third is connected with terms

which, as ilustrated in Figs. 6, 7 and 8, can make significant contributions to the governing equations.

Formulation procedure

To explain the significance of developing equations of motion by initially treating B as capable of assuming *any* position within the N_1–N_2 plane, as indicated in Fig. 4, we begin with some observations underlying this approach. Typically, when discretizing a continuum by using the assumed modes method, one employs modes obtained from the classical solution of a problem geometrically similar to the one at hand. For example, for the analysis of the behavior of a beam attached to a rigid block rotating about an inertially fixed axis, as shown in Fig. 10, the modal functions associated with the free vibrations of a fixed cantilever beam would be used. For the beam B, using modes obtained from the analysis of a longitudinally fixed beam would thus appear to be appropriate; however, the utilization of such modes entails several undesirable consequences. Since the position of B changes constantly, the modes would have to be regarded as time-dependent. This is objectionable because the fixed beam modes cannot be obtained analytically, which means that a simulation of motions of B would require their numerical generation at each integration time step. Furthermore, terms in the equations involving definite integrals of the modal functions would not be constants, as in eqns (22) and (31), but would be functions of time that also would have to be evaluated at every integration step. The use of these modes is thus seen to engender severe computational burdens.

One alternative to working with classical modes is simply to invent modes which satisfy the boundary and support conditions but can be expressed in analytical form. Such modes are still time-dependent, but need not be generated numerically. The arbitrariness of this approach, however, renders it unattractive.

The method used to develop eqn (70) permits one to reduce computational costs to a minimum by regarding the beam as unrestrained at that point of the analysis where modes are introduced. Since no time-dependent support conditions arise in connection with an unrestrained beam, the modes can be taken to be time-independent, as are the $\phi_i (i = 1, \ldots, \nu)$ of eqn (1). Consequently, it becomes unnecessary to generate modal functions and associated definite integrals at each step of a numerical simulation. The cost of this benefit is the necessity of introducing the two otherwise unnecessary quantities z_2 and θ (see Fig. 4).

Modal functions

Even when working with the time-independent modal functions of eqn (1), one has considerable latitude in the choice of their form and number. Two considerations

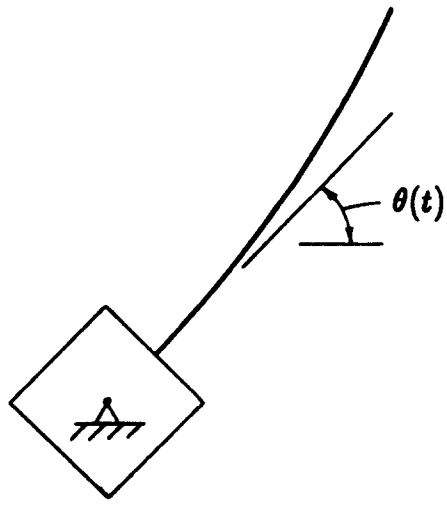

Fig. 10. Rotating beam and block.

influencing the selection of the modal functions are physical relevance and analytical convenience. The modal functions of eqn (99) are sound in both of these respects. Table 1 indicates the excellent agreement between classically obtained frequencies of free vibrations and those obtained by using unrestrained beam modes. Additionally, most of the constants a_{ij}, c_i, d_i, and $h_{ij}(i, j = 1, \ldots, \nu)$ of eqns (22) and (31) vanish.

The procedure used here to determine the number of modes necessary to generate an accurate simulation has been to select a reasonable number of modes, perform the desired simulation, perform the simulation again using one more mode, and compare results. If the results agree sufficiently well, the former number of modes is accepted as being adequate. If not, the procedure is repeated. In this way, four modes have been found to be acceptable in generating the responses shown in Figs. 2 and 3, and five modes have been found to be acceptable for Figs. 6, 7 and 8.

Longitudinal inertia forces

The significant differences between Figs. 6, 7 and 8 are attributable to retaining nonlinear expressions in the kinematical analysis leading to eqn (70). This fact is relevant to other beam problems ultimately described by linear equations of motion derived via Kane's method or Lagrange's equations. For example, for the problem of a four-bar mechanism with elastic links, considered in [14], terms reflecting inertia forces that give rise to "transverse elastic restoring forces due to axial loading" are introduced artifically by treating the *inertia* forces as *active* forces obtained from potential functions. By way of contrast, the corresponding terms of the present analysis appear automatically in the generalized *inertia* forces when complete kinematical expressions are used at the outset.

REFERENCES

1. S. Timoshenko, D. H. Young, and W. Weaver, Jr., *Vibration Problems in Engineering*, 4th Ed., Wiley, New York (1974).
2. C. D. Mote, Jr., A study of band saw vibrations, *J. Frankl. Inst.* **279**, 430–444 (1965).
3. G. G. Adams and H. Manor, Steady motion of an elastic beam across a rigid step. *J. Appl. Mech.* **48**, 606–612 (1981).
4. B. Tabarrok, C. M. Leech, and Y. I. Kim, On the dynamics of an axially moving beam, *J. Frankl. Inst.* **297**, 201–220 (1974).
5. E. Coddington and M. Levinson, *Theory of Ordinary Differential Equations*, McGraw-Hill, New York (1955).
6. C. S. Hsu, On the parametric excitation of a dynamic system having multiple degrees of freedom, *J. Appl. Mech.* **30**, 367–372 (1963).
7. L. Meirovitch, *Analytical Methods in Vibrations*, Macmillan, New York (1967).
8. T. R. Kane, *Dynamics*, 3rd Ed., Stanford University, Stanford, CA (1972).
9. C. W. Wampler, K. W. Buffinton, and J. Shu-hui, Formulation of equations of motion for systems subject to constraints, *J. Appl. Mech.* (In press).
10. T. R. Kane and D. A. Levinson, Simulation of large motions of nonuniform beams in orbit, part II—the unrestrained beam, *J. Astronaut. Sci.* **229**, 245–275 (1981).
11. C. R. Wylie, *Advanced Engineering Mathematics*, 4th Ed., McGraw-Hill, New York (1975).
12. L. Meirovitch, *Methods of Analytical Dynamics*, McGraw-Hill, New York (1970).
13. A. D. S. Barr, Dynamic instabilities in moving beams and beam systems, *Proc. 2nd Int. Congr. Theory of Machines and Mechanisms* **1**, 365–374, Zakopane, Poland (1969).
14. G. H. Sutherland, Analytical and experimental investigation of a high-speed elastic-membered linkage, *J. Eng. Ind.* **98**, 788–794 (1976).